Waveguide Based Relative Permittivity Measurement System for Axion Dielectric Haloscope

Moinak Nath

[a] *Fermi National Accelerator Laboratory (Science Undergraduate Laboratory Internship) Summer 2023*
[b] *Northwestern University*

Abstract

We discuss dielectric haloscopes as a way to detect axions, which are a promising candidate for dark matter. Building a dielectric haloscope is a medium term goal of the Broadband Reflector Experiment for Axion Detection (BREAD) collaboration at Fermilab. We discuss the theory behind this new design and potential advantages of the new design. In order to build an accurate dielectric haloscope, we must first build an apparatus to accurately measure the complex relative permittivity and loss tangent of dielectric materials. We then present a summary of the major relative permittivity measurement methods and explain why we chose a waveguide based system. We give an overview of the major ways to extract the relative permittivity from measured scattering parameters (obtained from a Vector Network Analyzer) including the method of least squares, the Nicholson-Ross-Weir method, and the NIST iterative method. Our waveguide based relative permittivity measurement setup is presented. We discuss Network Analyzer calibration and simulations of the measurement setup that were run in Ansys HFSS. Simulated and measured S-parameter data from a WR-42 waveguide are shown. Finally, we present a measurement of the permittivity of Rogers TMM3 materials as well as simulations of the measurement process for Rogers TMM4 and Teflon materials.

1. Introduction

Axions are a hypothetical particle which are a strong candidate for dark matter. These particles arise from the Peccei-Quinn solution to the strong charge-parity problem [5]. The strong-CP problem arises from quantum chromodynamics, which predicts that charge and parity symmetry violation should be possible. A system has charge symmetry when flipping the signs of all the charges does not change the system and a system has parity symmetry when flipping the position axes does not change the system. However, charge-parity symmetry violation has never been found in any experiment conducted so far [3]. To account for this phenomenon, Peccei and Quinn introduced the axion field, which can be thought of locally as a classical field oscillating with a frequency proportional to the mass of the axion particle [6], [9].

BREAD (Broadband Reflector Experiment for Axion Detection) is an axion search. The main detector has a cylindrical geometry with a parabolic mirror. The cylindrical metal barrel converts dark matter into photons, which is then focused by the parabolic mirror into a photo sensor [7]. Our project concerned the dielectric haloscope, an alternative detector, which consists of a stack of dielectrics, a mirror, a focusing lens, and a receiver [6].

In the dielectric haloscope, the system of photons, axions and currents is described by a Lagrangian density. From the Lagrangian density, we can derive the Euler-Lagrange equations of motion for the system. These equations of motion lead to a set of equations which can be recognized as a modified form of Maxwell's equations [6].

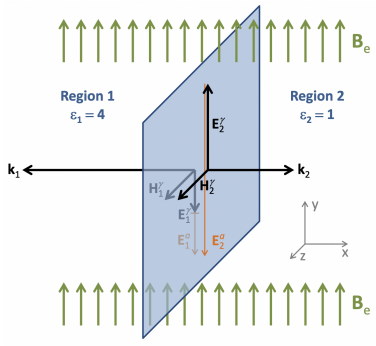

Figure 1: Diagram of a boundary between two dielectrics under a strong external magnetic field. Note the electromagnetic wave emitted in both directions, represented by $\mathbf{k_1}$ and $\mathbf{k_2}$.

At an interface between two dielectric materials and under a strong magnetic field, continuity of the electric and magnetic fields, combined with the modified Maxwell's equations, implies a propagating EM wave traveling in both perpendicular directions. Hence, dielectric haloscopes can detect axions under a strong external magnetic field. Each dielectric boundary emits a wave (caused by axion)

and the power builds up through the stack, so that the output wave can be detected by the receiver [6].

The unique design of the dielectric haloscope allows greater flexibility and a wider axion mass search range than traditional cavity resonators. For example, the spacings between the dielectric layers can be tweaked to allow for a larger signal boost and mass range. The height of the layers can similarly be adjusted for even greater control. With the dielectric haloscope design, a mass search range of 40-400 μeV becomes feasible [6]. Cavity resonators would need to be very small to measure such high frequencies.

2. Complex Relative Permittivity

The complex relative permittivity, ϵ_r, of a material can be obtained by eq. (1) :

$$\epsilon_r = \epsilon_r^{'} - j\epsilon_r^{''} \tag{1}$$

The loss tangent is simply the ratio of the imaginary part of the permittivity to the real part of the permittivity:

$$\tan\delta = \frac{\epsilon_r^{''}}{\epsilon_r^{'}} \tag{2}$$

Relative permittivity is a frequency dependent complex quantity whose real part is the dielectric constant and whose imaginary part represents how much like a conductor the material is. The loss tangent shows how lossy a medium is [2].

The power of the emitted wave in the haloscope depends on the indices of refraction of the dielectric materials at the boundary. Since the index of refraction is related to the complex permittivity by:

$$n = \sqrt{\epsilon_r} \tag{3}$$

for non-magnetic materials.

Thus the power of the emitted wave depends on the relative permittivity of the materials used [6]. If the loss tangent is too high, the wave will be absorbed by the dielectrics and axion detection will be impossible. Thus, to design an effective dielectric haloscope, we need a way to measure the relative permittivity and loss tangent of dielectric materials. This was the focus of our project.

3. Relative Permittivity Measurement Systems

3.1. Measurement Methods

There are many different methods to characterize the complex relative permittivity of dielectric materials. The best method depends on the frequency range, material shape, material phase, lossiness, and temperature. These include coaxial probe, cavity resonator, free-space, and transmission line or waveguide methods. A rich literature exists on relative permittivity measurement methods. An extensive literature review was conducted on the various methods.

Almost all of the methods involve using a Vector Network Analyzer to measure the scattering parameters of the device under test (DUT). Physically, the S-parameters are interpreted as the reflection (S_{ii}) and transmission coefficient (S_{ij}). Once the S-parameters of the measurement apparatus are measured, the material properties must be extracted [2].

In coaxial probe methods, which are ideal for liquids or semi-solids, a cut off section of a transmission line is submersed in the Material Under Test (MUT). The probe is connected to a Vector Network Analyzer where a one port measurement is performed of S_{11}. These methods are non-destructive and broadband but have limited accuracy for low loss media [11].

In resonator methods, a cavity with a high quality factor is constructed. Inserting a dielectric inside the resonator will change the resonant frequency and quality factor of the cavity. The permittivity is calculated using the resonant frequency before and after the MUT is inserted. This method is robust at cryogenic temperatures and permittivity extraction is relatively easy. The biggest flaw of these methods is that they are good for measuring the permittivity at a single frequency or a very narrow frequency range. Another major flaw, which was especially important for us, was the fact that in order to reach the high-GHz or THz frequency range, a resonator would have to be extremely small, so much so that constructing one in the lab is impractical [4], [11].

In the transmission line method, the MUT is placed inside a waveguide or coaxial airline, and the complex permittivity is extracted for reflection and transmission measurements. This method has the major advantage of being broadband, but has the disadvantage that the sample must be prepared to fit inside the waveguide or coaxial airline [8], [11].

Since the goal of BREAD is to search a wide frequency range for axions, we needed a method that is broadband. We also wanted a method that could feasibly go to terahertz range frequencies and be cooled to cryogenic tem-

peratures in the future. To this end, we implemented the waveguide method for relative permittivity measurement because it is broadband and can handle relatively high frequencies.

3.2. Extraction Methods

Another literature review was conducted on permittivity extraction techniques. Permittivity extraction is a difficult process, but all the methods are different ways of solving a system of complex-valued equations. There is also a least squares method, where theoretical formulas for the S-parameters are compared with the measured data and the program finds the permittivity of best fit [2].

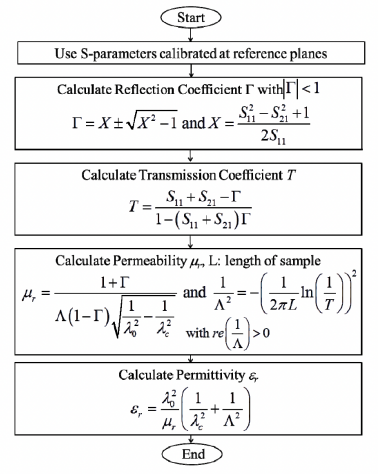

Figure 2: An overview of the Nicholson-Ross-Weir extraction process [8].

The Nicholson-Ross-Weir (NRW) method is convenient because it provides an almost closed form solution for the permittivity and permeability based on just S_{11}, S_{21}, the waveguide cutoff frequency (λ_c), the free space frequency (λ), and the sample length L. A summary of this extraction method is shown in Figure 2. A major problem with this method is that when calculating $\ln(\frac{1}{T})$, the correct branch must be selected since the complex logarithm is defined as follows:

$$\ln\left(\frac{1}{T}\right) = \ln\left(\frac{1}{|T|}\right) + j(\theta + 2\pi n) \tag{4}$$

where $\theta = \arg(\frac{1}{T})$ and $n \in \mathbb{Z}$. Selecting the correct value of n is a major challenge when using the NRW algorithm. The NRW method also breaks down when the sample length is a multiple of the half-wavelength of microwave radiation in the sample [2].

The National Institute of Standards and Technology has developed several iterative methods for permittivity extraction [10]. These methods depend on finding the root of a complex-valued equation using the Newton-Raphson numerical method.

First, we must introduce the propagation constant in air (the empty waveguide) γ_0:

$$\gamma_0 = j\sqrt{(\frac{\omega}{c})^2 - (\frac{2\pi}{\lambda_c})^2} \tag{5}$$

whereas the propagation constant (γ) in the material is defined as:

$$\gamma = j\sqrt{\epsilon_r\epsilon_0\mu_0\omega^2 - (\frac{2\pi}{\lambda_c})^2} \tag{6}$$

assuming that the magnetic permeability $\mu_r = 1$. Now, the reflection coefficient (Γ) in the material is found as:

$$\Gamma = \frac{\gamma_0 - \gamma}{\gamma_0 + \gamma} \tag{7}$$

again under the assumption that the material is nonmagnetic. Finally, the transmission coefficient in the material is given by:

$$T = e^{-\gamma L} \tag{8}$$

where L is the sample length. Once the aforementioned quantities are calculated, the permittivity can be extracted by numerically solving equation (9):

$$S_{11}S_{22} - S_{21}S_{12} + e^{-2\gamma_0(L_{air}-L)}\frac{T^2 - \Gamma^2}{1 - T^2\Gamma^2} = 0 \tag{9}$$

(L_{air} is the length of the waveguide) using the Newton-Raphson method [1].

4. Methods

4.1. Laboratory Setup

In the laboratory, we constructed a measurement setup consisting of a WR-42 Rectangular Waveguide, 2 Waveguide to Coaxial adapters, a Rohde & Schwarz ZVA-24 Vector Network Analyzer (VNA), and a sample of Rogers TMM3 dielectric material (see Figure 3).

A piece of the sample (L = 6.21 mm) wass inserted into the waveguide, which was attached to the VNA via 2 Waveguide to Coaxial adapters. Before insertion, the sample was milled, then sanded to fit inside the waveguide. The VNA measures the S-parameters of the waveguide setup, which can be used to extract the relative permittivity of the materials. We measured the S-parameters in a frequency range of 18-24 GHz. The S-parameters from the WR-42 waveguide filled with Rogers TMM3 can be seen in Figure 3.

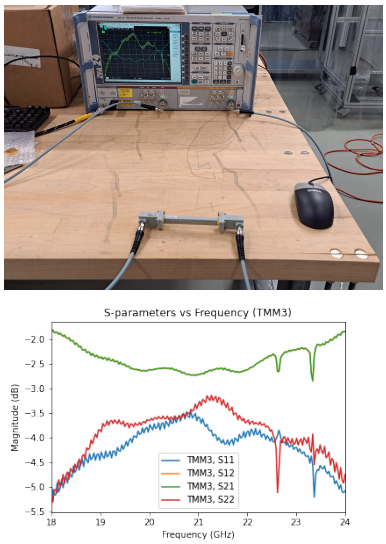

Figure 3: The upper panel shows a picture of the laboratory setup. The lower panel shows the S-parameters obtained from Rohde & Schwarz ZVA-24 Vector Network Analyzer with Rogers TMM3 material in waveguide

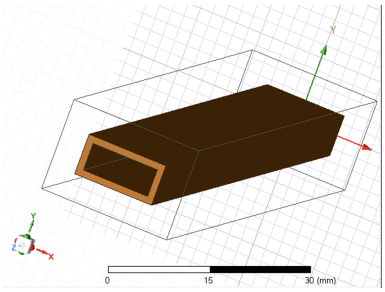

Figure 4: 3D model of a WR-42 waveguide constructed in Ansys HFSS

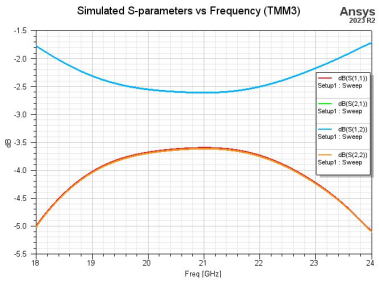

Figure 5: Simulated S-parameters of WR-42 waveguide filled with Rogers TMM3 material

4.2. VNA Calibration

The Rohde & Schwarz VNA was calibrated using the Through-Reflect-Line method. The calibration required a short and a ¼ waveguide shim for insertion between the two waveguide to coaxial adapters. First, the short was inserted between the adapters and the S-parameters were measured. Next, the two adapters were connected to each other and the S-parameters were measured. Finally, the ¼ waveguide shim was inserted between the two adapters and the S-parameters were measured. Calibration calculations were performed using a calibration kit (.ck) file, which automates a rather messy process.

4.3. Simulations

The WR-42 rectangular waveguide was modeled in Ansys HFSS. The 3D model was filled with TMM3 ($L = 6.21$ mm) and TMM4 ($L = 2.54$ mm). A model of the WR-90 waveguide was filled with Teflon ($L = 11.75$ mm). The modeling process consisted of creating a 3D model of the copper waveguide, creating an airbox around the waveguide, and applying port boundary conditions (see Figure 4). The program then provided simulated S-parameters, as shown in Figure 5. The same 18-24 GHz frequency range was used in all simulations except for Teflon, where we used a range of 8-12 GHz.

4.4. Extraction

Extraction of the material properties from the S-parameters was attempted via the Nicholson-Ross-Weir (NRW) Algorithm, which was coded in Python. We had limited success with this method, since selecting the correct branch of the natural log proved quite difficult. The code was tested to work with n = 0, but it could not accurately select other values of n. Additionally, the inaccuracy peaks at half wavelengths were also an issue.

We successfully implemented a version of the NIST method using SciPy's Newton function, which solves equation (9) using the Newton-Raphson root finding algorithm.

5. Results

As a sanity check, we first extracted the dielectric properties of air. As expected, we got a dielectric constant very close to 1 and a loss tangent that was close to zero. These results are presented in Figure 6.

Rogers Corps advertises their TMM3 Laminate with process dielectric constant of 3.27 and a design dielectric constant of 3.45. Our measurement of the real part of the permittivity aligns well with this advertised value for the design dielectric constant. The simulation was run with the process dielectric constant of 3.27 and that result also aligns well with our expectations. In the loss tangent data, we observe a much higher loss than predicted by the simulation. It should be noted that there is quite a bit of noise in the loss tangent measurement. These results are presented in Figure 7.

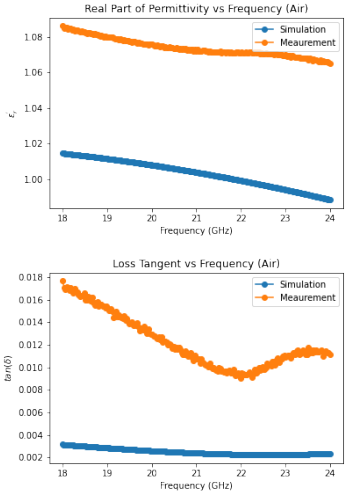

Figure 6: The upper panel shows the simulated (blue) and measured (orange) dielectric constant of air. The lower panel shows the simulated (blue) and measured (orange) loss tangent of air.

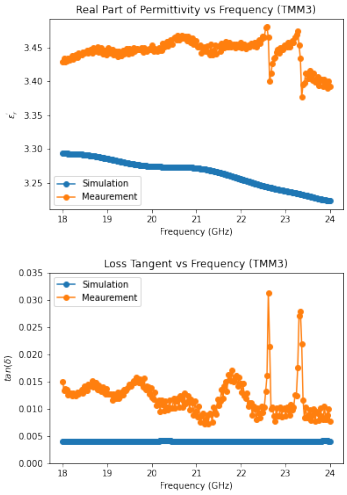

Figure 7: The upper panel shows the simulated (blue) and measured (orange) dielectric constant of Rogers TMM3. The lower panel shows the simulated (blue) and measured (orange) loss tangent of Rogers TMM3.

Finally, we ran two more simulations of Rogers TMM4 and Teflon. Both simulations produced results produced dielectric constants in line with the expected values: 4.50-4.70 for TMM4 and 2.1 for Teflon. These results are presented in Figure 8 and Figure 9.

In all the results, the dielectric constant decreases or stays relatively constant as frequency increases. This is expected as the dielectric constant generally decreases with frequency.

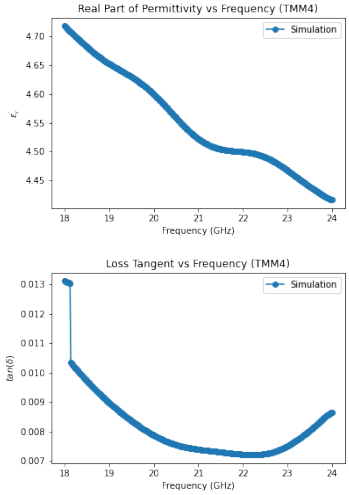

Figure 8: The upper panel shows the simulated dielectric constant of Rogers TMM4. The lower panel shows the simulated loss tangent of Rogers TMM4.

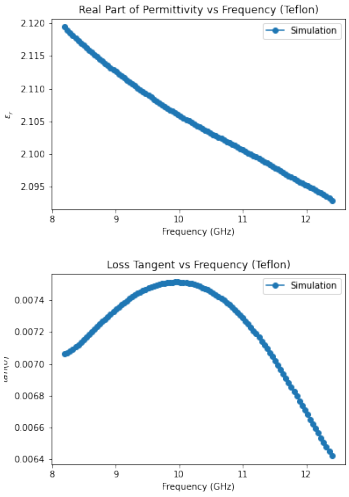

Figure 9: The upper panel shows the simulated dielectric constant of Teflon. The lower panel shows the simulated loss tangent of Teflon.

6. Conclusion

Now that we have a working method of measuring the permittivity, the next step is to try to make the method more accurate by attempting to improve the calibration and cable quality. Additionally, building a fixture for the waveguide apparatus to limits its movements may improve accuracy, as even minute movements can cause noise.

An analysis of uncertainty in the permittivity measurements, as outlined in [2] is also an important next step. After perfecting the measurement at room temperature, we need to explore how to cool the apparatus to cryogenic temperatures. Once this is done, work can begin on designing a dielectric haloscope. This project was an important first step towards the ambitious goal of building a

working dielectric haloscope.

References

[1] J. Baker-Jarvis, E. Vanzura, and W. Kissick. Improved technique for determining complex permittivity with the transmission/reflection method. *IEEE Transactions on Microwave Theory and Techniques*, 38(8):1096–1103, 1990. doi: 10.1109/22.57336.

[2] L.-F. Chen. *Microwave electronics: Measurement and Materials Characterization*. Wiley, 2004.

[3] M. Creutz. Cp violation in qcd, 2018.

[4] J. Krupka. Measurements of the complex permittivity of microwave circuit board substrates using split dielectric resonator and reentrant cavity techniques. *Seventh International Conference on Dielectric Materials, Measurements and Applications [Preprint]*, 1996. doi: 10.1049/cp:19960982.

[5] J. Liu, K. Dona, G. Hoshino, S. Knirck, N. Kurinsky, M. Malaker, D. W. Miller, A. Sonnenschein, M. H. Awida, P. S. Barry, and et al. Broadband solenoidal haloscope for terahertz axion detection. *Physical Review Letters*, 128(13), 2022. doi: 10.1103/physrevlett.128.131801.

[6] A. J. Millar, G. G. Raffelt, J. Redondo, and F. D. Steffen. Dielectric haloscopes to search for axion dark matter: theoretical foundations. *Journal of Cosmology and Astroparticle Physics*, 2017(01):061–061, January 2017. doi: 10.1088/1475-7516/2017/01/061.

[7] A. J. Millar, G. G. Raffelt, J. Redondo, and F. D. Steffen. Dielectric haloscopes to search for axion dark matter: Theoretical foundations. *Journal of Cosmology and Astroparticle Physics*, 2017(01):061–061, 2017. doi: 10.1088/1475-7516/2017/01/061.

[8] V. H. Nguyen, M. H. Hoang, H. Phan, T. Hoang, and T. Vuong. Measurement of complex permittivity by rectangular waveguide method with simple specimen preparation. volume 2015, 10 2014. doi: 10.1109/ATC.2014.7043419.

[9] R. D. Peccei. The strong CP problem and axions. In *Lecture Notes in Physics*, pages 3–17. Springer Berlin Heidelberg, 2008. doi: 10.1007/978-3-540-73518-2_1.

[10] R. . Schwarz. *Measurement of Dielectric Material Properties*.

[11] K. Technologies. Basics of measuring dielectrics, August 2019.